

## Conceptual design of prestressed slab bridges through one-way flexural load balancing

Marcello Arici<sup>a</sup> and Michele Fabio Granata\*

*Università di Palermo, DICAM, Viale delle Scienze, Palermo, Italy*

*(Received March 19, 2013, Revised October 30, 2013, Accepted November 1, 2013)*

**Abstract.** In this paper a study on prestressed concrete slab bridges is presented. A design philosophy based on the concept of load balancing through prestressing is proposed in order to minimize the effects of delayed deformations due to creep. Aspects related to the stress redistribution inside these bridges for time-dependent phenomena are analyzed and discussed, by applying the principles of aging linear visco-elasticity. Prestressing is seen as an equivalent external load which counterbalances the permanent loads applied to the bridge, nullifying the elastic deflections due to sustained loads, and thus avoiding the related delayed deformations. An optimization of the structural behavior through the use of one-way prestressing is achieved. The determination of a convenient variable depth of slab bridges and the correspondent layout of tendons is considered as a useful means for applying the load balancing concept in actual cases of structures like long cantilevers or bridge decks. A case-study related to the slab bridges built 30 years ago at Jeddah in Saudi Arabia is presented and discussed, in order to show the effectiveness of the proposed approach to the conceptual design of prestressed concrete bridges.

**Keywords:** slab bridges; prestressing; flexural load balancing; variable cross section; creep; delayed deformations; funicular structures

---

### 1. Introduction

The arch and the beam have completely different structural behaviors. The arch has a mainly axial behavior due to the geometric curvature, while the beam has a mainly flexural behavior. Prestressed concrete members integrate both aspects, thanks to an intelligent mutual collaboration between concrete and steel. Prestressed concrete structures are traditionally dimensioned and checked on the basis of the construction stages, within the hypothesis of elastic linear behavior of materials. Particularly the analysis is performed in the initial phase (in which a minimum value of bending moment occurs) and in the final one (in which a maximum value of bending moment occurs), with the aim of a full exploitation of concrete and prestressed steel strengths. This design philosophy implies a quasi-permanent flexural stress associated to an elastic curvature which maintains all concrete sections under a worthless state of stress. By contrast durability should be assured through a minimal and “natural” state of stress, for which concrete sections are always

---

\*Corresponding author, Assistant Professor, E-mail: [michelefabio.granata@unipa.it](mailto:michelefabio.granata@unipa.it)

<sup>a</sup>Professor, E-mail: [marcello.arici@unipa.it](mailto:marcello.arici@unipa.it)

subjected to an uniform compression, with temporary deviations from this state, due to the effect of live loads. This is the typical behavior of funicular arches. This leads to another design philosophy, opposite to the previous one, for which flexural stresses have to be balanced, with the immediate healthy consequence of reducing elastic and delayed deformations. Concrete is indeed characterized by rheological behavior which implies long-term delayed deformations. Creep of concrete occurs when concrete members are subjected to sustained loads and it is due to the breakage and reformation of bonds at various highly stressed sites within the colloidal microstructure of the calcium silicate hydrate gels in the hardened cement paste (Jirásek and Bažant 2002). This phenomenon is concomitant with shrinkage, which implies increasing shortening of concrete members with time but can also produce cracking stresses when it is restrained. Rheological properties of concrete are apparently secondary aspects in the analysis of structures but they can have a fundamental role in prestressed structures, long cantilevers, large roofing and bridges, influencing structural behavior and durability for a long time in service life.

Prestressing can limit, reduce or control the effects of these rheological properties of concrete as well as it can balance the flexural state of stress. Integral prestressing (or full prestressing) was introduced by Freyssinet in 1928 (Bernard-Gély and Calgaro 1994), who lays the foundations for this new material establishing the general principles, that are nowadays still valid. Although simple prestressed structures were built before the 2<sup>nd</sup> World War, the first important bridge built by this technique was the Luzancy bridge in 1946 and later many others built for the reconstruction of bridges in Europe. The possibility of obtaining prestressed structures in which small values of tensile stresses are admitted was due to Ulrich Finsterwalder, who stated the concept of so-called “limited prestressing” (Leonhardt 1964). Afterwards Abeles introduced the partial prestressing concept, through which the concrete section can undergo significant tensile stresses (Abeles 2003), but cracking is strongly limited by optimizing the degree of prestressing. In this last case prestressing is in aid of the ordinary steel of reinforced concrete sections (Walther 1982). Partial prestressing has been extensively investigated and a useful review of this technique can be found in Naaman (1985) as well as in Ghali and Tadros (1985). Recommendations on partially prestressed structures are given by the American Concrete Institute (ACI 1999). Today external prestressing with unbonded tendons (Naaman 1990) is rapidly spreading for new constructions and for the rehabilitation and retrofitting of existing ones; many interventions with external prestressing have been made for strengthening existing deteriorated bridges and this technique provides an efficient solution for a wide range of bridge typologies.

The technological development, with the use of precast segments and different launching methods, with respect to the classical centrings, allows prestressing to be used extensively in the field of concrete bridges. The majority of segmental bridges (Mathivat 1979, Granata and Arici 2013) or incrementally launched bridges (Arici and Granata 2007, Granata *et al.* 2013b) with box concrete sections are built by using full or limited internal prestressing (Recupero and Granata 2013). Moreover cable-stayed bridges are often built with prestressed concrete decks (Arici *et al.* 2011) for medium span lengths.

Prestressing allows engineers to design structures by balancing the load, by modifying boundary conditions and by creating supports within the structure. An example of this philosophy in designing bridges is the Neckar viaduct at Weitingen, built in 1978, where the side spans are twice as long as the central ones, thanks to the external cables that supply an internal additional support, avoiding the presence of piers grounded on the valley slopes (Leonhardt 1986). The same solution was adopted in the Osomort viaduct, built in 1995 (Aguilò *et al.* 2004), in which every span is supported by bottom external tendons deviated at the midspan. A concept similar to the

strip post-tensioning of flat slabs was adopted instead in the Hradec Kralove bridge, a curved slab bridge in which transverse prestressing compensates for the cantilever deformation of the wide deck (Strasky 2003), supplying internal additional supports in the transverse section of the bridge.

Prestressing can be seen not only as an imposed mutual deformation between the tendon and the concrete member, which generates a compressive state of stress, but also as an equivalent load applied to the structure which can compensate external loads (Arenas de Pablo 1974, Oh and Jeon 2001). The load balancing concept was developed by Lin (1963) and Leonhardt (1964), and it was originally conceived for strength capacity design (Van der Molen 1999) and afterwards also applied to evaluation of deflections (Gilbert and Mickleborough 2005) of structures with partial, limited or full prestressing. Chiu *et al.* (1996) applied these concepts to segmental bridges built by cantilevering, in order to control excessive deflections. The load balancing concept is based on the fact that during post-tensioning, the structure is loaded by an equilibrium of forces, inducing a state of stress and deformation that can change due to the effects of creep (Strasky 2003). In this connection, concrete structures are different from steel ones because during construction and in service life stresses are redistributed due to concrete creep and the layout of prestressing tendons markedly influences the global behavior and ultimate capacity of the structure.

As a consequence large structures in which these effects are relevant are hard to design because the stresses change in time and the target of the designer is to achieve an initial stage of a structure in which this redistribution of stresses is minimized. This requirement can be fulfilled by using internal or external prestressing which compensates for the dead load, creating a reduced state of elastic deformation at the end of construction (Favre and Markey 1994). If this approach is followed, then the creep delayed flexural deformations, which are proportional to the initial elastic ones, are reduced and the overall redistribution of stresses is limited. The limitation of creep delayed deformations plays a fundamental role in the design of large structures, as shown by the authors in previous studies about concrete and composite cable-stayed bridges (Granata *et al.* 2012a) or concrete arch bridges built by suspended cantilevers (Granata *et al.* 2012b) and by lattice cantilevers (Granata *et al.* 2013c), for which prestressing is employed in temporary and definitive stays, adopting an appropriate sequence of cable stressing in the construction stages.

The load balancing method was applied to redundant structures, especially to continuous beams (Lin and Thornton 1972). The main methodology for the determination of the tendon layout in a redundant structure is the concordant tendon one, which was established by Guyon (1960). Afterwards different researchers addressed the problem of tendon layout optimization in continuous beams (Stern 1999). Ng and Kwan (2006) developed a methodology for tendon optimization for curved bridges through the load balancing method, while Aalami (1990) presented a study in which load balancing is used for the determination of the tendon layout in structures with sudden variations in cross section and in non-prismatic slabs. Moreover 1-way and 2-way flat slabs have been studied in order to compensate permanent loads on slabs by internal prestressing (Lin and Burns 1982). Kuyucular (1991) presented an algorithm for prestressing optimization, with the aim of minimizing prestressing steel in concrete slabs. Teixeira and Assan (1998) analyzed continuous prestressed slabs using the finite element method (FEM), indicating design criteria for prestressing tendon optimization. Khan *et al.* (2010) applied the load balancing method to 1-way prestressed slabs with FEM analyses and recently the same authors extended their studies to 2-way prestressed slabs (Khan *et al.* 2013).

In this paper the load balancing method is applied to prestressed concrete slab bridges, for which a particular tendon configuration of internal prestressing can induce a good level of dead load counterbalance with a resulting state of uniform compression for sustained loads and a related

limitation of deflections. The proposed approach for load balancing of concrete slab bridges is based on one-way prestressing and it is substantially different from those reported in the literature: in the present case load balancing is achieved on slabs with variable depth, by optimizing the depth variation of the concrete cross section, with a chosen tendon layout. By balancing external loads with one-way prestressing it is possible to nullify external actions and consequently the bi-dimensional state of stress and strain in the slab. Effects of creep on delayed deformations are considered and the effectiveness of load balancing is shown both for the serviceability and ultimate limit states. The case-study of the slab bridges designed by the author and built at Jeddah, Saudi Arabia (Arici 1985), is discussed and the implications of load balancing are underlined in reference to the durability of these bridges, built about 30 years ago.

## 2. Effects of creep in prestressed concrete structures

Let us consider a concrete beam subjected to a sustained distributed load applied at time  $t_0$ . The initial elastic deformation  $\varepsilon_e(t_0)$  increases as time goes by, due to the delayed deformations, through the so-called creep function  $J(t, t_0)$ , which represents the total strain at time  $t$  due to a unitary stress applied at  $t_0$

$$\varepsilon_\sigma(t) = \sigma_c(t_0) J(t, t_0) = \varepsilon_\sigma(t_0) [1 + \varphi(t, t_0)] = \sigma_c(t_0) \frac{1 + \varphi(t, t_0)}{E_c(t_0)} \quad (1)$$

where  $\varphi(t, t_0)$  is the creep coefficient, which gives the creep deformation rate and is supplied by international codes (ACI 2008, fib 2012);  $E_c(t_0)$  is the Young modulus of concrete at the time of load application and  $\sigma_c(t_0)$  is the stress related to the elastic deformation. A more complete explanation of creep effects on prestressed concrete structures and of creep predictive models can be found in Chiorino (2005), through the aging linear viscoelastic approach, and in the ACI documents (ACI 2012).

If compressive stresses are below 40-50% of concrete strength, then the principle of superposition for sustained loads applied to the structure in different subsequent times (intervals  $d\sigma_c$ ) can be used and the total deformation is given by the following integral equation

$$\varepsilon_c(t) = \sigma_c(t_0) J(t, t_0) + \int_{t_0}^t J(t, \tau) d\sigma_c(\tau) \quad (2)$$

which is strictly valid for rheological homogeneous structures with rigid restraints, by disregarding stress-independent strains (due for example to shrinkage and temperature).

Eq. (2) states that a structure with these properties subjected to sustained loads modifies its state of deformation by increasing it through the creep function, the stress state being invariable or variable only for the subsequent increments  $d\sigma_c$  due to additional sustained loads. If a redundant structure is subjected to sustained imposed deformations, the reciprocal integral equation can be written:

$$\sigma_c(t) = \varepsilon_\sigma(t_0) R(t, t_0) + \int_{t_0}^t R(t, \tau) d\varepsilon_\sigma(\tau) \quad (3)$$

in which the relaxation function  $R(t, t_0)$  represents the total stress at time  $t$ , due to a unitary imposed deformation applied at time  $t_0$ . The relaxation function decreases with time and it can be

found starting from the creep function, by solving a Volterra integral equation. Eq. (3) states that a structure subjected to sustained imposed strains modifies its stress state by decreasing it through the relaxation function, the elastic deformations being invariable or variable only for the subsequent increments  $d\varepsilon_\sigma$  due to additional imposed deformations.

For rheological homogeneous structures with rigid restraints for which changes in the static scheme occur (for example during construction), the principle of acquisition of the modified static system can be stated as follows: “in a structure subjected to sustained loads at time  $t_0$ , whose initial static system is modified into a final structural system by the introduction of additional restraints at time  $t_1 > t_0$ , the system of the stresses (stresses, internal forces and external reactions) evolves for  $t > t_1$  and approaches the system of the stresses corresponding to the application of the loads to the structure in its final structural system” (ACI 2012).

As a consequence of this principle, stresses and strains evolve in time. The redistribution of stresses is due to the fact that every point of the structure increases its deformation due to creep after the application of sustained loads; if a restraint prevents these creep deformations at a generic time  $t_1$ , a reaction arises in the added restraint, which is a function of time  $t$ , depending on the deformations prevented in time. Stress resultants and restraint reactions can be expressed as a linear combination of the stresses obtained in the elastic scheme of the structure subjected to the sustained load before the addition of the delayed restraint (stress resultants or restraint reactions  $S_0$ ) and after the addition of the delayed restraint (stress resultants or restraint reactions  $S_1$ )

$$S(t) = S_0 + (S_1 - S_0) \xi(t, t_0, t_1) \tag{4}$$

The coefficient of this linear combination is given by the value of the redistribution function  $\xi(t, t_0, t_1)$  at time  $t$ . This is an increasing function which has value  $\xi=0$  for  $t \leq t_1$ , assuming the value  $\xi=1$  for the total acquisition of the modified scheme (this is a limit condition that is approached but not reached). The redistribution function is related to the creep and relaxation functions through the following Volterra integral equation

$$\xi(t, t_0, t_1) = \int_{t_1}^t R(t, \tau) dJ(\tau, t_0) \tag{5}$$

which can be solved by numerical methods. Graphs or design aids giving the values of redistribution functions are available in international recommendations or in specialized literature and web sites ([www.polito.it/creepanalysis](http://www.polito.it/creepanalysis)). An approximate value of the redistribution function can be found through the Age-Adjusted Effective Modulus Method (AAEM) proposed by Bažant (Bažant 1972, Jirasek and Bažant 2002)

$$\xi(t, t_0, t_1) \cong [\varphi(t, t_0) - \varphi(t_1, t_0)] E_c(t_1) / [(1 + \chi(t, t_1) \varphi(t, t_1)) E_c(t_0)] \tag{6}$$

where  $\chi(t, t_1)$  is the so-called aging coefficient, which varies between the values of 0.6 and 1.0, and which can be approximated for practical applications to the mean value 0.8.

If the delayed restraint is added at time  $t_1 = t_0^+$ , very close to the time of load application, soon after the initial elastic deformation occurs, then the redistribution function becomes

$$\xi(t, t_0, t_0^+) = 1 - \frac{R(t, t_0)}{E_c(t_0)} \tag{7}$$

The stress history for a structure with a variable static scheme is expressed by Eq. (4); the history of deformations is expressed instead by the following relation

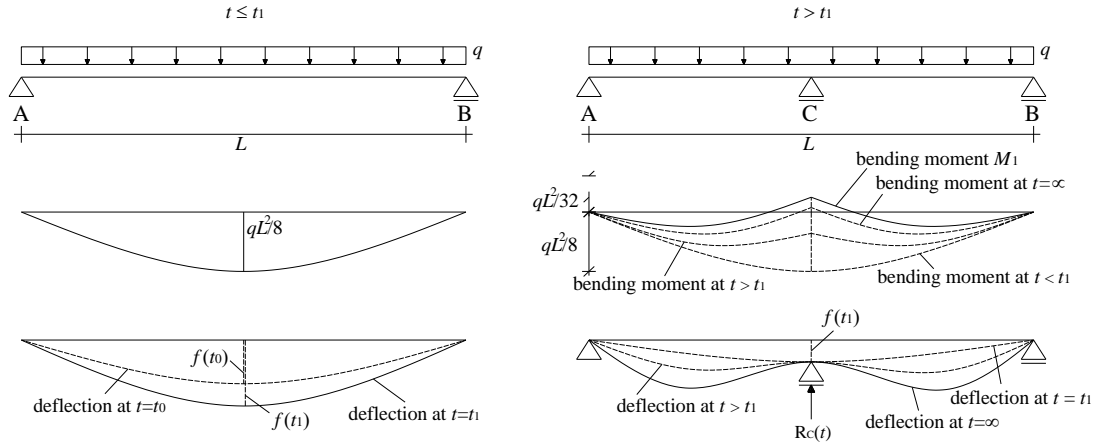


Fig. 1 Example of a structure with a variable static scheme. Initial configuration of simply supported beam and final scheme with intermediate support

$$D(t) = D_0 [1 + \varphi(t_1, t_0)] + D_1 [\varphi(t, t_0) - \varphi(t_1, t_0)] \tag{8}$$

where  $D_0$  is the generic deformation (displacement, rotation, etc) evaluated in the initial elastic scheme while  $D_1$  is the generic deformation evaluated in the modified elastic scheme with the added restraint.

As an example of a structure with a variable static scheme, consider a simple supported beam, which is subjected to a distributed sustained load applied at time  $t_0$ , and in which an intermediate support is added at time  $t_1 > t_0$  (Fig. 1). The evolution of stresses and strains in the structure is given by Eqs. (4) and (8). If  $M_0$  and  $M_1$  are the values of the bending moments at each section of the beam in the elastic schemes without and with the delayed restraint, the history of the bending moment is

$$M(t) = M_0 \quad \text{for } t \leq t_1$$

$$M(t) = M_0 + (M_1 - M_0) \xi(t, t_0, t_1) \quad \text{for } t > t_1 \tag{9}$$

while the history of the deflections is

$$D(t) = D_0 [1 + \varphi(t, t_0)] \quad \text{for } t \leq t_1$$

$$D(t) = D_0 [1 + \varphi(t_1, t_0)] + D_1 [\varphi(t, t_0) - \varphi(t_1, t_0)] \quad \text{for } t > t_1 \tag{10}$$

Although these principles are strictly valid for rheological homogeneous structures, when designers have to deal with inhomogeneous structures, due to the presence of steel elements (composite structures) or to different cast properties of concrete segments, the same principles can still be considered valid in order to evaluate the global structural behavior. Moreover the uncertainties due to the evaluation of average environmental conditions and to the dispersion of data supplied by predictive creep models, affect the design of structures under the effects of time-dependent phenomena (Granata *et al.* 2013a).

In the beam of the previous example (Fig. 1) the central support is added soon after the

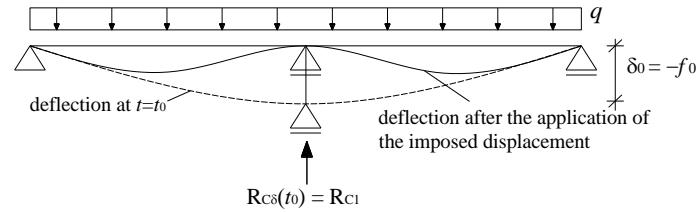


Fig. 2 Delayed restraint forced up to the initial value of deflection

application of a sustained load, so the principle of acquisition of the modified static scheme has to be applied. At the time of restraint addition, the reaction of the added support is zero. Afterwards the support reaction  $R_c$  grows from zero to a time-dependent value at the generic time  $t > t_1$ , due to the rise of delayed deflections prevented in the restrained section. Reaction  $R_c$  follows the law of stress redistribution given by Eq. (4)

$$R_c(t) = R_{c1} \xi(t, t_0, t_0^+) = R_{c1} \left( 1 - \frac{R(t, t_0)}{E_c(t_0)} \right) \quad (11)$$

where  $R_{c1} = 5/8 \cdot qL$  is the reaction at the intermediate support in the final elastic scheme of the continuous beam, being  $R_{c0} = 0$  in the initial elastic scheme. The maximum value of the reaction is achieved at the final time of analysis ( $t_\infty$ ). As shown in Fig. 1 the bending moment over the support grows with the same law, approximating (without reaching) the value related to the final elastic scheme ( $M_{c1} = -1/32 qL^2$ ).

Let us imagine now that this support is forced upward (for example by a hydraulic jack) at the same time  $t_0^+$ , with an imposed displacement that is equal to the deflection  $f(t_0)$ . This operation clearly corresponds to the application of an imposed deformation  $\delta = -f(t_0)$  in the modified scheme (Fig. 2) and consequently the stress values induced by this imposed displacement decrease in time with the relaxation function (Eq. (2)). In this way at time  $t_1 = t_0^+$  a reaction  $R_{c\delta} = R_{c1}$  suddenly appears in the intermediate restraint. By applying the principles of linear viscoelasticity, the value of the restraint reaction in time, due to the change in the static scheme and to the application of the upward imposed deformation is the following one

$$R_c(t) = R_{c1} \xi(t, t_0, t_0^+) + R_{c\delta}(t_0) \frac{R(t, t_0)}{E_c(t_0)} = R_{c1} \left( \xi(t, t_0, t_0^+) + \frac{R(t, t_0)}{E_c(t_0)} \right) = R_{c1} \left( 1 - \frac{R(t, t_0)}{E_c(t_0)} + \frac{R(t, t_0)}{E_c(t_0)} \right) = R_{c1} \quad (12)$$

Eq. (12) states that the reaction value is invariable in time and that no stress redistribution occurs if the added delayed restraint is forced up to the value of the restraint reaction that in the final elastic scheme would be subjected to the sustained load.

In this way the application of the viscoelastic principles permits one to obtain a structure in which soon after the change in restraints, internal forces instantaneously achieve the values that they would have in the modified scheme if the load was applied on it at the initial time  $t_0$ . This fact allows engineers to take advantage of creep for appropriately modifying the behavior of concrete structures, because in this case the states of stress and strain are independent from time and from uncertainties due to the creep predictive model adopted.

If the delayed restraint is forced at a time  $t_1 = t_0 + \Delta t$  ( $\Delta t$  being a wide time range of some

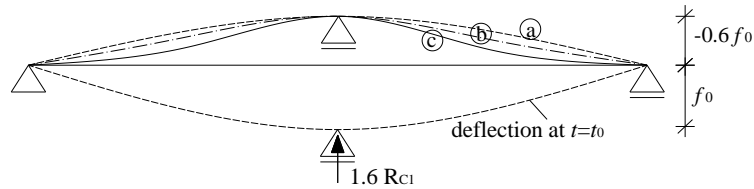


Fig. 3 Delayed restraint forced up to a value that is 1.6 of initial deflection: a) deflection due to the imposed displacement at  $t = t_0^+$ ; b) deflection at  $t > t_0^+$ ; c) deflection at final time  $t_\infty$

weeks or months), the value of reaction  $R_c(t)$  does not remain unchanged in time, because it would vary with the function  $[\xi(t, t_0, t_1) + R(t, t_1)/E_c(t_1)]$ . So the condition to avoid stress redistribution is the application of the imposed deformation soon after the time of a delayed restraint addition, being very close to the time of sustained load application.

When the delayed restraint is forced up to a value that is different to the one of the continuous beam, the redistribution of stresses differs from the previous one. Let us imagine forcing the restraint with an imposed displacement that is 1.6 times the initial elastic deflection:  $\delta = -1.6 f(t_0)$ ; in this way, all the total sustained load  $Q = qL$ , is balanced by the jacking force  $1.6 R_{c1} = qL$  and a camber is given to the beam, eliminating downward displacements (Fig. 3). Then the intermediate support reaction would be  $R_{c\delta}(t_0) = 1.6 R_{c1}$  and the history in time of the restraint reaction would become

$$R_c(t) = R_{c1} \xi(t, t_0, t_0^+) + 1.6 R_{c1} \frac{R(t, t_0)}{E_c(t_0)} = R_{c1} \left( 1 + 0.6 \frac{R(t, t_0)}{E_c(t_0)} \right) \quad (13)$$

decreasing from the time of application to the final time of analysis ( $t_\infty$ ). It is worth noting that the time function  $R(t, t_0)/E_c(t_0)$ , when  $t_0 = 28$  days and  $t = 365$  days (after one year and under average external and concrete conditions) is less than half of its initial value, initially decreasing very fast and after slowly till  $t_\infty$ . Consequently internal forces like bending moment and shear would follow the same law, quickly approaching the configuration of the continuous beam. Fig. 4 shows the variation in bending moments in the beam without forcing the added restraint, with an imposed upward displacement  $\delta = -f(t_0)$  and with an imposed displacement  $\delta = -1.6 f(t_0)$ . It can be seen that the effect of redistribution due to creep is always that of approximating the bending moment diagram related to the continuous beam with the delayed restraint as it would be applied at the time of load application. In the case of the unforced restraint, the stress redistribution increases the negative bending moment value, while in the case of the imposed displacement  $\delta = -1.6 f(t_0)$ , the stress redistribution approximates the value in the final scheme by decreasing the moment on the support (Fig. 4). The bending moments remain unchanged when  $\delta = -f(t_0)$ . Hence, this configuration can be assumed as the “natural” configuration, to which the structure tends with time; the concept of a structural natural configuration can be recognized in Strasky (2003).

This behavior demonstrates that the natural distribution of internal forces (associated to the modified system) is always approximated, due to creep. This occurs independently from the starting condition and from the value of the imposed displacement  $\delta = -\beta f(t_0)$ , with  $0 \leq \beta \leq 1.6$ , though the degree of the modified system recover depends on creep, relaxation and redistribution functions. For  $\beta=1$  the structure is not subjected to stress redistribution and the final modified

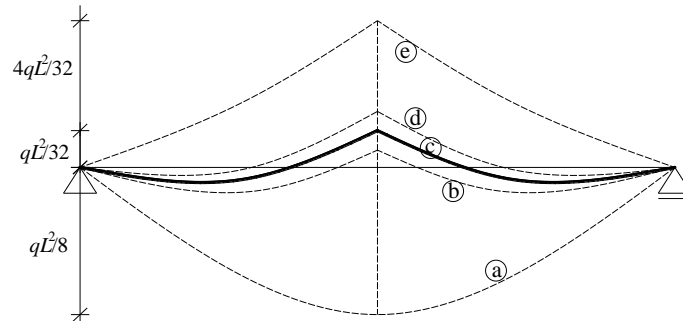


Fig. 4 Stress redistribution of bending moments: (a)  $t = t_0$ , (b) unforced delayed restraint at final time  $t_\infty$ , (c) forced delayed restraint at  $t = t_0^+$ , equivalent to the continuous beam, (d) time  $t_\infty$  with the restraint forced to  $1.6 f(t_0)$ , (e) time  $t = t_0^+$  with the restraint forced to  $1.6 f(t_0)$

system is perfectly achieved; for  $\beta=0$ , the delayed restraint is not forced up and the history of stresses and deformations changes with Eqs. (4) and (8), while for  $\beta=1.6$ , redistribution of stresses proceeds with Eq. (13). If an intermediate value of  $\beta$  is considered (for example  $\beta=1.2$ ) it means that the restraint is forced up to a displacement that is greater than the initial deflection  $f(t_0)$  and redistribution due to creep takes the bending moment towards the final modified system.

As pointed out before, one year after restraint addition, the excess of deformation ( $0.2 f(t_0)$ ) is reduced to less than one half and afterwards it decreases very slowly till  $t_\infty$ . In the next section it will be shown that this situation is equivalent to the application of prestressing in a structure in which the value  $(\beta-1)$  represents the percentage of prestressing losses.

### 3. Additional supports supplied by prestressing and time-dependent losses

Limited or full prestressing can be adopted to reduce or avoid tensile stresses in concrete elements and to eliminate the effects of delayed deformations. Partial prestressing can be adopted to limit cracking stresses in reinforced concrete, inserting the necessary amount of ordinary reinforcements (Naaman 1980). Moreover through prestressing forces it is possible to change restraints and to create intermediate supports in the structure. This possibility is evident in cable-stayed bridges where stays suspend the deck, creating elastic intermediate supports, but similar results can be achieved by inserting internal or external post-tensioned tendons in girder bridges as in the cited cases of Neckar, Osomort and Hradec Kralove bridges. In these structures the global behavior is always affected by shrinkage and creep and the previous principles have to be applied.

Let us now consider the simply supported beam described in the previous section and substitute the intermediate support through an external or an internal tendon whose slope is given by  $\tan \theta = 2e_c/L \cong \sin \theta$ , with a deviator in the midspan section (Fig. 5).

If the friction losses are disregarded, the overall effect of instantaneous losses of prestressing can be taken into account by assuming the actual value of compressive force transferred to the concrete element as  $P_0 = T - \Delta T$ , in which  $T$  is the jacking force and  $\Delta T$  the value of instantaneous losses. Afterwards the effect of delayed losses has to be considered and the final value of compressive force in the beam is  $P = P_0 - \Delta P_\infty$ , where  $\Delta P_\infty$  is the total value of delayed losses due

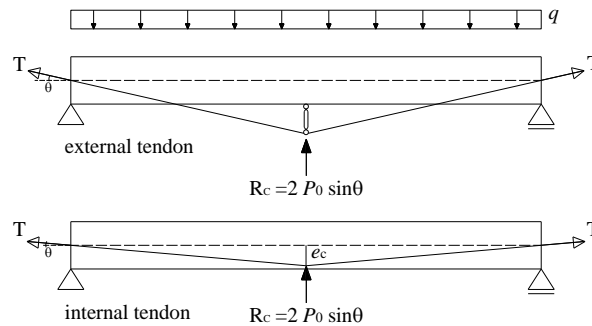


Fig. 5 Support supplied by prestressing tendons

to shrinkage, creep and steel relaxation. When the jacking value of force  $T = P + \Delta T + \Delta P_\infty$  is applied to the tendon, in the intermediate section a reaction  $R_c(P) = 2P \cdot \sin \theta$  occurs, after a long time ( $t_\infty$ ). If this value is equal to the reaction  $R_{c1}$  of an intermediate support in the equivalent continuous beam subjected to the sustained load  $q$ , the effect of prestressing is equal to the delayed rigid restraint added in the example of the previous section. When  $R_c(P) = R_{c1}$  the structure depicted in Fig. 5 is actually the same as the one depicted in Fig. 2. As a consequence, the elastic deflection of the sustained load is entirely recovered by the upward displacement of prestressing and the resulting displacement of the intermediate point is nullified. The distribution of bending moments in the beam is the same as the equivalent continuous beam with two equal spans and the final situation corresponds to the curve (c) of Fig. 4. Moreover, the effect of the prestressing force is also a compressive stress introduced in every section of the beam, which is helpful for eliminating the danger of cracking.

Note that at the time of prestressing force application, if the jacking force is  $T$ , the initial compressive force is  $P_0$  and it is different from the final value  $P$  after losses are exhausted. If  $P$  is dimensioned to give the reaction value  $R_{c1}$  at the intermediate section, the upward displacement is greater than the deflection due to the load. This fact is healthy for the beam because the upward displacement simplifies detachment from the formwork; afterwards the losses reduce the value of the upward displacement and of the vertical reaction as time goes by, approaching the configuration of the continuous beam with the intermediate rigid support. If the value of prestressing force  $P$  in service life (time  $t_\infty$ ) is dimensioned in order to equal the value of reaction  $R_{c1}$  of a rigid support and the total losses  $\Delta P_\infty$  are evaluated, then the initial value of prestressing force is  $P_0 = P + \Delta P_\infty = \beta P$ , and the reaction  $R_c(P)$  depends on  $\beta$ . Hence the coefficient  $\beta$  which gives the level of prestressing losses is equivalent to the coefficient  $\beta$  of the forced restraint, previously seen. The final result of a beam subjected to the prestressing force  $P_0$ , with the tendon configuration of Fig. 5, is a continuous beam with an intermediate support that has an initial small pre-camber and an almost null value of displacement in the central section when prestressing losses are exhausted. The final stress state is very close to that of the continuous beam. During the service life of the beam, the initial camber quickly decreases due to the double effect of losses and the relaxation of the imposed deformation, approaching the “natural” condition of the continuous beam with an intermediate support.

The value of delayed prestressing losses in time can be written in the following way (ACI 2012, Tadros *et al.* 1975, CEN 2005)

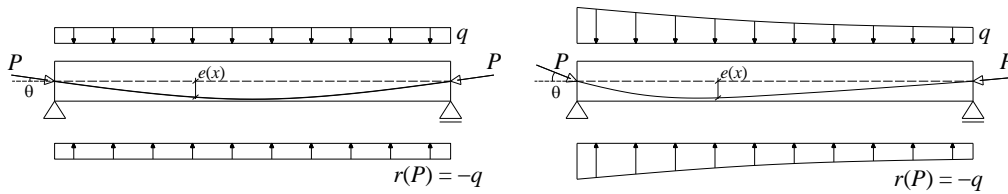


Fig. 6 Load balancing of uniform and non uniform distributed loads through curved tendons

$$\Delta P(t_\infty) = A_p \frac{n_0 f_{c0} \varphi(t_\infty, t_0) + \varepsilon_{sh}(t_\infty) E_p + f'_{re}(t_\infty)}{1 + n_0 \rho_p k_p [1 + \chi \varphi(t_\infty, t_0)]} \quad (14)$$

where  $n_0 = E_p/E_c(t_0)$  is the ratio between elastic moduli of the prestressing steel and concrete;  $\rho_p = A_p/A_c$  is the ratio between the areas of the prestressing tendons and the concrete cross-section;  $k_p = 1 + e^2/r_c^2$  is the contribution of the tendon eccentricity  $e$  with respect to the centroid of the cross-section, and  $r_c$  is the radius of inertia of the concrete cross section;  $f_{c0} = P_0/A_c(1 + e^2/r_c^2) = P_0/A_p \rho_p k_p$ , is the compressive stress in the concrete fibre next to the prestressing steel tendon;  $\varepsilon_{sh}(t)$  is the shrinkage strain at the time  $t$  with respect to the time of prestressing application;  $f'_{re}(t)$  is the steel stress variation due to the reduced relaxation ( $f'_{re} = 0.8 f_{re}$ ) and  $\chi$  is the aging coefficient. In fact, the delayed strain in the concrete fibre next to the steel reinforcement is the sum of three components, due respectively to creep, shrinkage and steel relaxation. The histories of internal forces and deformations in time, due to the delayed prestressing losses, are obtained and shown in Granata *et al.* (2013a).

#### 4. Load balancing concept and funicular structures

In the previous cases the value of deflection is nullified at one point in the structure, by inserting an additional support in that point through the rational optimization of the tendon layout and the prestressing force, also considering losses. The same can be done along the entire beam if a curved tendon is used, so that the value of the resultant deflection, the sum of the applied load and of prestressing, can be nullified in each section (Fig. 6). Hence the external load can be perfectly balanced by prestressing, obtaining a continuous support along the beam. This is the so-called load balancing concept, whereby prestressing can be seen as an equivalent load opposite to the external ones.

In this connection when in a beam with constant section, the tendon is arranged by following the funicular curve of load  $q$ , this generates an equivalent load  $r(P)$  which counterbalances the external load, nullifying the elastic deflections due to load  $q$ . The presence of load  $r$ , which directly nullifies the distributed load  $q$ , and of the concentrated forces at the tendon anchorages, generates a line of compressive resultant forces in the beam which coincides with the geometric axis, establishing funicular behavior, as occurs for the thrust line of an arch. If the balanced structure is considered axially rigid (assuming that axial deformations do not occur), bending moment and shear force are nullified in each section and only an axial force with uniform compressive stresses in the cross section is obtained. This result can be achieved both for uniform and non-uniform distributed loads (Fig. 6), by varying the eccentricity  $e(x)$  of the tendon with

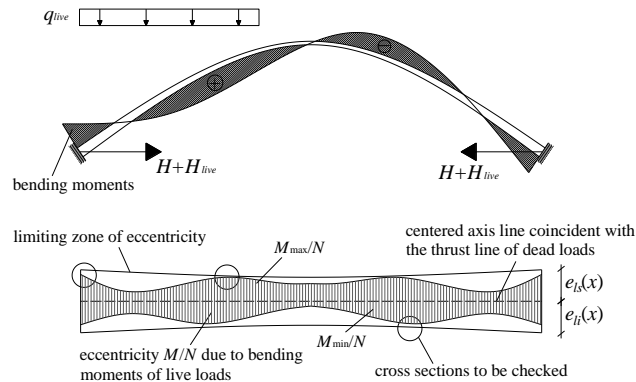


Fig. 7 Arch with non symmetric live loads and eccentricity diagrams due to bending moments

respect to the geometric axis of the element and by choosing the right prestressing force value:  $P = M_{max}/e_{max}$ .

The behavior of the funicular beam with complete flexural load balancing can be assimilated to the axially rigid arch behavior. Indeed in prestressed members, the horizontal component of prestressing force has the same role as is played by the thrust  $H$  of an arch, with the difference that prestressing is artificially induced by the designer while the arch thrust is a natural effect due to the geometric curvature and to the boundary conditions (Guyon 1960). In axially rigid funicular arches the geometric axis coincides with the thrust curve of the permanent load and the eccentricity between them is given by the effects of variable loads (moving loads of bridges, temperature, etc.). So funicular arches only present bending moments and shear forces for the effects of live loads, thrust loss due to axial deformation and delayed strains due to creep. The increased value of thrust  $H_{live}$  in a funicular arch, due to live loads, adds to the value  $H$  due to the permanent load and the thrust line must enter the limit diagram, without inducing tensile stresses. Fig. 7 shows an example of an arch subjected to a non-symmetric live load and the limit field of compressive force eccentricity along the entire arch. The diagram of the maximum and minimum moments for service loads is depicted, scaled to the axial force  $N$  of each section, and it is superimposed on the diagram of the central inertia core of cross sections (limiting zone), in order to control the maximum values of eccentricity and tensile stresses.

Analogously with the case of the arch, the prestressed beam can be designed with the aim of balancing all permanent loads at time  $t_{\infty}$ . In a bridge they are the self-weight, additional loads due to pavement, guardrails, footpaths, etc. If the beam has a variable cross section, the self-weight is not uniformly distributed along the beam and the tendon configuration has to be chosen with caution considering the variable eccentricity between the tendon and the geometric axis line. If concentrated loads are applied to the bridge, the eccentricity line can present slope discontinuities, while the tendon layout must be as smoother as possible, avoiding points with high concentrated friction losses. For variable cross sections, it is possible to modify not only the tendon layout but also the law of cross section variation, in order to achieve an eccentricity line that compensates for the external loads (Fig. 8). In this way it is possible to define a “funicular structure”, that is a structural member with an optimal geometric shape which permits the flexural load balancing with a smooth layout of tendons. These results can be achieved with a convenient disposition of restraints, assuring the condition of allowing longitudinal displacements due to axial forces of

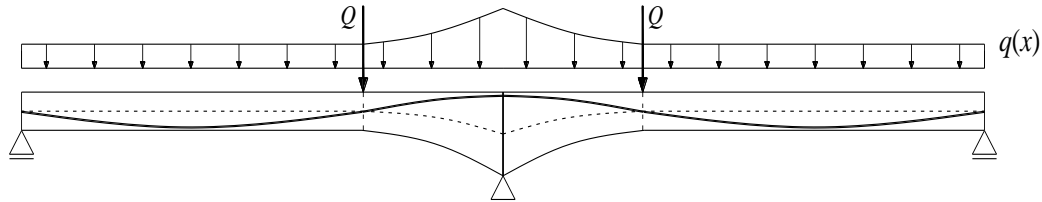


Fig. 8 Beam with variable cross section, distributed and concentrated loads

prestressing and to temperature effects. In the funicular structure, bending moment, shear force and flexural deflections are zero in each section. For permanent loads only a uniform compressive stress remains into the structural member because shear force and bending moments are nullified. This fact corresponds to a new origin of the stress state in the cross section, established for permanent loads, for which the value of tensile or compressive stresses due to additional live loads has to be added to this state (Arenas de Pablo 1974). This situation is mainly related to service limit state.

If the funicular shape is chosen for a bridge, applying all permanent loads, a successive study is required for live loads, especially for the maximum and minimum effects of moving loads, from the points of view of both serviceability and ultimate limit state (Favre and Burden 1999). Researches on the flexural capacity at the ultimate limit state for prestressed structures with bonded and unbonded tendons can be found in Lee and Kim (2011).

In order to establish the acceptable level of tensile stresses related to environmental conditions, it is also necessary to consider the action of repetitive loads on the bridge and the consequent strength to fatigue. In a motorway bridge it has been estimated that only 25-40% of the maximum moving load value is reached with a frequency that could cause fatigue problems to concrete and steel (Leonhardt 1980). This is because the cycle loads of these bridges act with reduced intensity with respect to the maximum value supplied by international codes. As a consequence, in order to guarantee that no fatigue problems occur in the structure during service life, a good design condition is to limit tensile stresses to zero for 50% of the maximum value of moving loads, allowing a limited value of tensile stresses for higher loads, which has to be faced by ordinary steel reinforcement.

If the load balancing concept is applied and the bridge geometric shape is chosen together with the tendon layout, the deflection is automatically limited, as shown above and it is not necessary to consider additional cambers in order to compensate for delayed deflections due to creep. Indeed, when the initial elastic deflection of sustained loads is balanced by the effect of prestressing, the structure has negligible flexural deflections and consequently negligible delayed deflections. This approach to design is especially suitable for structures with large cantilevers, such as a sports stadium, platform roofs or wide bridge decks.

In the following sections these concepts are applied to the design of concrete slab bridges.

It has to be noted that, even though a slab bridge is a bi-dimensional structure, for which a bi-dimensional state of stress and strain is established under external loads, through one-way prestressing it is possible to counterbalance external loads. In this connection, by inserting a one-way prestressing the external load is nullified and in the slab the related states of flexural stress and strain are nullified in every direction.

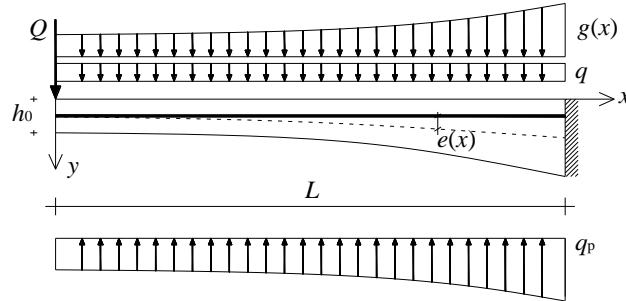


Fig. 9 Load balancing with straight tendons for a cantilever with variable depth

## 5. Flexural load balancing of prestressed concrete slab bridges

The case of a concrete cantilever beam that is equivalent to a slab strip, 1.0 meter wide, with total length  $L$ , is considered. It has a rectangular cross section, with variable depth  $h(x)$  and a horizontal extrados. Prestressing tendons are inserted with different layouts. The aim of the analysis is to find the geometric profile of the slab which assures perfect balancing, through one-way prestressing, of bending strains due to the dead loads applied. This result can be achieved by compensating for the self-weight  $g(x)$ , a constant uniformly distributed load  $q$  (which is related to superimposed dead loads like pavements) and a concentrated load  $Q$  placed at the free end (Fig. 9).

### 5.1 Load balancing with straight tendons and variable depth

Let  $\gamma$  be the weight per unit volume of concrete and  $h_0 = h(0)$  the depth of the initial cross section, being the  $x$  axis being set as in Fig. 9. Let  $P$  be the prestressing force in the tendon in service life for which all time-dependent losses are exhausted and friction is disregarded, by considering the value of  $P$  constant along the tendon. Because the centroids of the cross sections are placed on a curved line, the eccentricity of the prestressing force varies at every section according to the following law:  $e(x) = [h(x) - h_0]/2$ .

The external distributed load that is equivalent to prestressing  $q_p(x)$  is expressed by the relation

$$q_p(x) = -P \frac{d^2 e(x)}{dx^2} = -\frac{P}{2} \frac{d^2 h(x)}{dx^2} \quad (15)$$

The equilibrium condition between dead loads applied to the beam and prestressing action is

$$q_p(x) + g(x) + q = 0 \Rightarrow \frac{P}{2} \frac{d^2 h(x)}{dx^2} - \gamma h(x) - q = 0 \quad (16)$$

Eq. (16) is a differential equation of the 2<sup>nd</sup> order whose solution is

$$h(x) = A \sinh \alpha x + B \cosh \alpha x - \frac{2q}{P\alpha^2} \quad (17)$$

where  $\alpha^2 = 2\gamma/P$  while  $A, B$  are constants to be found through the boundary conditions

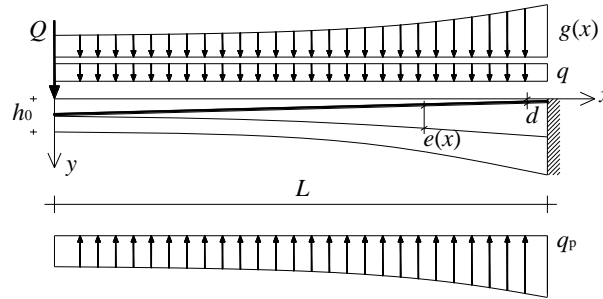


Fig. 10 Load balancing with inclined straight tendons for a cantilever with variable depth

$$\left. \frac{de}{dx} \right|_{x=0} = \frac{Q}{P} \Rightarrow A = \sqrt{\frac{2Q^2}{\gamma P}} ; \quad h(0) = h_0 \Rightarrow B = h_0 + \frac{q}{\gamma} \quad (18)$$

The solution which gives the geometric profile  $h(x)$  of the cantilever beam or slab with variable depth, assuring the perfect balancing of dead loads  $g$ ,  $q$  e  $Q$  with prestressing  $P$ , is expressed by the following relation

$$h(x) = \sqrt{\frac{2Q^2}{\gamma P}} \sinh \alpha x + \left( h_0 + \frac{q}{\gamma} \right) \cosh \alpha x - \frac{q}{\gamma} \quad (19)$$

Eq. (19) gives the law of depth variation along the beam and the consequent eccentricity variation, with a straight horizontal tendon.

When instead the same condition has to be obtained with a straight inclined tendon (fig. 10), the same equation can be used, by imposing the related boundary conditions. The solution is given by the following law of the variable depth

$$h(x) = \left( \sqrt{\frac{2Q^2}{\gamma P}} - \sqrt{\frac{(h_0 - 2d)^2 P}{2\gamma L^2}} \right) \sinh \alpha x + \left( h_0 + \frac{q}{\gamma} \right) \cosh \alpha x - \frac{q}{\gamma} \quad (20)$$

where  $d$  is the covering thickness of concrete over the tendon in the final clamped section.

### 5.2 Load balancing with parabolic tendons

The same result of load balancing can be obtained with a different prestressing force value and a parabolic tendon layout (Fig. 11). In this case the expression giving the eccentricity between cross section centroid and tendon line is the following

$$e(x) = \left( \frac{h_0}{2} - d \right) \frac{x}{L} \left( 2 - \frac{x}{L} \right) + \frac{h(x) - h_0}{2} \quad (21)$$

The equilibrium condition in the vertical direction between dead loads and prestressing equivalent loads is

$$\frac{P}{2} \frac{d^2 h(x)}{dx^2} - \gamma h(x) - q + \frac{2P}{L^2} \left( \frac{h_0}{2} - d \right) = 0 \quad (22)$$

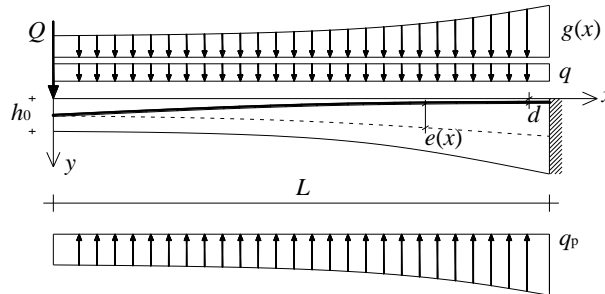


Fig. 11 Load balancing with parabolic tendons for a cantilever with variable depth

whose solution is

$$h(x) = A \sinh \alpha x + B \cosh \alpha x - \frac{q}{\gamma} - \frac{N}{\gamma L^2} (h_0 - 2d) \quad (23)$$

The related boundary conditions can be written as

$$\begin{aligned} \left. \frac{de}{dx} \right|_{x=0} &= \frac{Q}{P} \Rightarrow A = \sqrt{\frac{2Q^2}{\gamma P}} - \sqrt{\frac{2P(h_0 - 2d)^2}{\gamma L^2}} \\ h(0) &= h_0 \Rightarrow B = h_0 + \frac{q}{\gamma} + \frac{P(h_0 - 2d)}{\gamma L^2} \end{aligned} \quad (24)$$

The law of the variable depth which assures the perfect flexural load balancing effect is

$$h(x) = \left( \sqrt{\frac{2Q^2}{\gamma P}} - \sqrt{\frac{2(h_0 - 2d)^2 P}{\gamma L^2}} \right) \sinh \alpha x + \left( h_0 + \frac{q}{\gamma} + \frac{P(h_0 - 2d)}{\gamma L^2} \right) \cosh \alpha x - \frac{q}{\gamma} - \frac{P(h_0 - 2d)}{\gamma L^2} \quad (25)$$

Eqs. (19), (20) and (25) supply the depth variation  $h(x)$  of the cross section for different tendon layouts, the value  $P$  of the prestressing force being known.

The same equations can be used in an alternative way in order to find the most appropriate value of the prestressing force, once the geometric parameters  $h_0$ ,  $h(L)$  and  $d$  are known. The resulting value  $P$  of the prestressing force is the one which assures the perfect balancing of dead loads related to that geometry. Values of geometric parameters can be established through technological or mechanical conditions. For example, the minimum depth  $h_0$  can depend on the technological condition imposed by the actual size of the tendon anchorages or it can depend on the minimum depth which satisfies the local stress check of the slab under concentrated loads.

### 5.3 Effects of live loads and partial prestressing

A mechanical condition for the choice of the geometric shape is connected to the maximum allowable tensile stress in the concrete. The depth  $h(x_i)$  in the section  $x_i$  with the maximum value of tensile stress is strictly related to the considerations about allowable cracks in concrete. Let  $f_{ct}$  be the maximum allowable tensile stress and  $f_{ctk}$  the characteristic tensile strength of the concrete. The maximum value of tensile stress is defined as  $f_{ct} = f_{ctk}/\gamma_c$  in which  $\gamma_c$  is the partial safety factor. If

the designer choice is that of avoiding cracking, the value  $f_{ct}$  can be set to zero (full prestressing); when instead the designer choice is that of controlling crack width, a different value of  $f_{ct}$  could be considered. In both cases the maximum tensile stress in the section of height  $h(x_i)$ , after the live loads are applied, must satisfy the following condition

$$f_{\min} = \frac{P}{A_c} - \frac{M_{live}}{W_c} \geq -f_{ct} \tag{26}$$

where  $A_c$  is the effective concrete area of the cross section,  $W_c$  is the cross section strength modulus, and  $M_{live}$  is the bending moment due to live loads (moving loads and temperature).

By imposing  $f_{\min} = -f_{ct}$  and by setting  $f_{ct} = 0$ , in the case of a rectangular cross section, one obtains  $h(x_i) = 6M_{live}/P$ , while for a different value of  $f_{ct}$ , Eq. (26) is a 2<sup>nd</sup> order algebraic equation, written for the strip  $b = 1.00$  m wide

$$f_{ct}bh^2(x_i) + Ph(x_i) = 6M_{live} \tag{27}$$

whose solution is

$$h(x_i) = \frac{P}{2f_{ct}} \left( \sqrt{1 + \frac{24f_{ct}bM_{live}}{P^2}} - 1 \right) \tag{28}$$

which is the value of cross section depth that is consistent with the allowable tension value.

This is a convenient way to limit cracking in every cross section of the slab. From Eq. (28) a limit field can be obtained by considering the allowable eccentricity  $e_{lim}(x)$  related to the allowable tensile stress, in every section

$$e_{lim}(x) = \frac{h(x)}{6} \left( 1 + \frac{f_{ct}bh(x)}{P(x)} \right) \tag{29}$$

The such defined limit field corresponds to the limiting zone shown in Fig. 7.

If  $N(x)$  is the value of axial force at the generic section of abscissa  $x$ , the actual eccentricity of the compressive force  $M_{live}(x)/N(x)$ , must be less than the calculated limit eccentricity of each cross section ( $N(x)=P$  if the structure is statically determinate without other loads producing axial forces). The conditions to be checked for every combination of live loads in service life are

$$\left| e_{lim}^{inf}(x) \right| \geq \left| \frac{M_{live}^{min}(x)}{N(x)} \right| ; \quad \left| e_{lim}^{sup}(x) \right| \geq \left| \frac{M_{live}^{max}(x)}{N(x)} \right| \tag{30}$$

This evaluation has to be made for both positive and negative bending moments (i.e., for maximum and minimum values due to moving loads) and the two conditions of relation (30) must be simultaneously satisfied at each cross section.

In this way, in analogy with the procedure applied for the thrust line of the funicular arch (see section 4), the checking procedure to be carried out in order to avoid or limit cracking is illustrated in the flow chart in Fig. 12.

Concrete cracking can be controlled with different approaches:

(a) no tensile stresses are allowed in every section ( $f_{ct} = 0$ ) and cracks are completely avoided for every load combination (full prestressing).

(b) Tensile stresses are strongly limited for every load combination ( $f_{ct} = f_{ctk}/\gamma_c$ ) and temporary

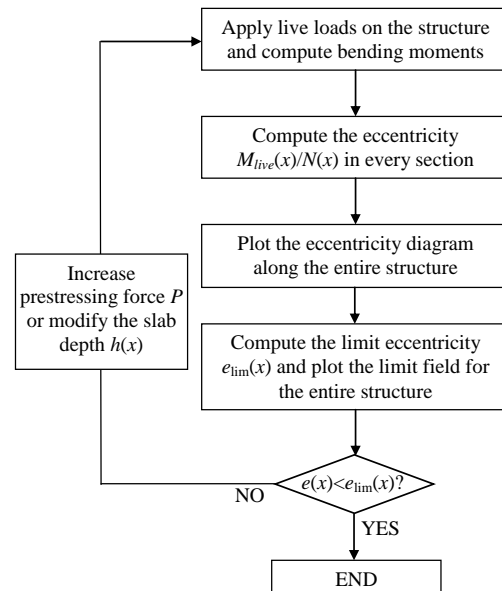


Fig. 12 Flow chart of structural check under live loads

micro-cracks could only appear for the maximum values of live loads: the serviceability limit state related to the first cracking is satisfied; micro cracks appear in a transient phase when live loads are applied and then they disappear, so steel corrosion is prevented (partial prestressing). In order to avoid fatigue problems due to the repetition of live loads, a null value of tensile stress is imposed for 40-50% of the maximum bending moment due to live loads (Leonhardt 1980).

(c) Tensile stress is not limited ( $f_{ct} = f_{ctk}$ ) but crack width is strongly limited to a value  $w = w_{max}$ . In this case the serviceability limit state related to crack opening has to be satisfied (Naaman 1985, Favre and Burden 1999). If cracks are allowed and open for the transient stage of maximum live load values, it is necessary to limit crack opening to a small value, preferably  $w_{max} = 0.1 \div 0.2$  mm, depending on the environmental conditions.

(d) Permanent bi-dimensional compression of every infinitesimal concrete element (as a kind of hydrostatic pressure) is achieved for the entire structure (i.e., prestressing in longitudinal and transverse directions assures compressive stresses in each direction), not allowing tensile stresses.

In cases b and c, in order to limit the crack width, tensile stresses have to be faced entirely through ordinary steel reinforcement.

In the following case-study the approach adopted was that of case b (partial prestressing with null tensile stresses for a percentage of live loads in order to control fatigue), applying approach d for the effects of permanent loads.

## 6. The case-study of the Jeddah slab bridges

### 6.1 Design of Jeddah bridges with the load balancing concept

The bridge designed and built over the Ruwais Lagoon at Jeddah (Fig. 13), Saudi Arabia, is the

first of several bridges, built in the first half of the 80s within a large-scale project concerning the “corniche”, a seafront boulevard running more than 30 km from the north to the south of the town (Arici 1985). It consists of a concrete slab bridge with five spans, each one 33.00 meters long with two side spans of 23.50 meters. The first bridge is horizontally curved with a constant radius of 600 m; the other ones are straight bridges. The deck is composed of a slender slab with a doubly variable depth. The longitudinal geometric shape of the bridge was determined through the load balancing method as a catenary shape. The geometric profile is symmetric and the maximum height of the deck over the lagoon sea level is about 10.00 meters.

The deck is 29.00 m wide with two carriageways composed of three lanes each, a central traffic island 3.00 m wide and two sidewalks 2.00 m wide. The deck is made of prestressed concrete slabs solidly joined to the piers and longitudinally connected by means of Gerber saddles. Each central pier supports a deck area of about 1000 square meters and the static configuration is that of an asymmetric cantilever supported by Gerber saddles. For each slab (33m×29m) longitudinal and transverse prestressing were provided to balance longitudinal and transverse bending moments due to dead loads. The cross section depth is longitudinally variable from 1.00 m (at the midspan) to 2.30 m (over the pier) and in the transverse direction from 0.32 m (at the free end) to 1.00 m (at the center).

The piers have a variable and nearly elliptical cross section and a total height of about 7.00 m. They were also vertically prestressed in order to face the deck torsion due to asymmetric loads on the deck, which is transferred to the pier as a bending moment by the rigid connection with the slab. The abutments are 29.00 m wide (like the deck, but they are not prestressed); elastomeric and neopot bearings are placed over the abutments and in the Gerber saddles, at the center of the cross section. The side transverse cantilevers are connected by steel shear pins.

The foundations are made of pyramidal footings each resting on 25  $\phi$ 600 piles of different lengths (not less than 20.00 m), driven into the soft soil of the lagoon and the coral cemented fragments layer, beneath.

In order to minimize the negative effects of the environmental conditions on the structure, the main design choice was to avoid stresses due to temperature and concrete cracking under dead loads (self-weight and superimposed permanent loads) and to maintain each section entirely

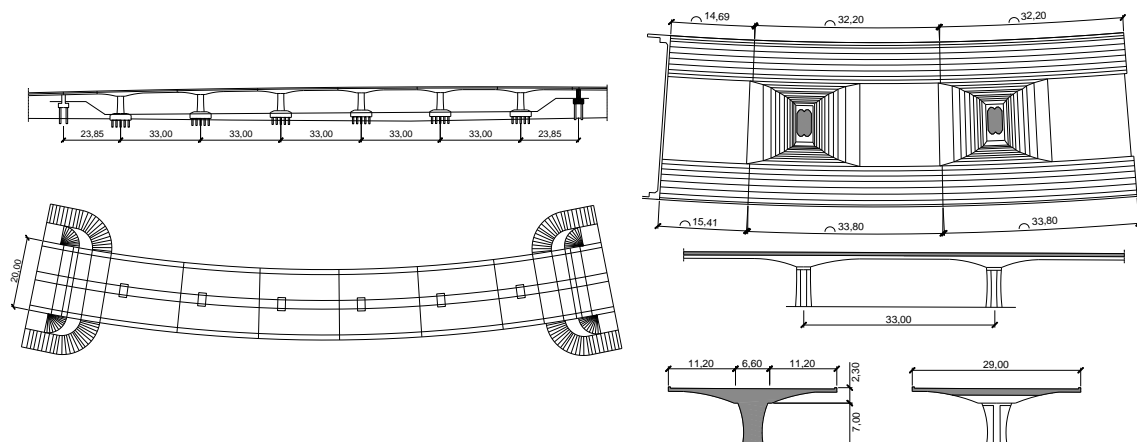


Fig. 13 Geometry of the first Jeddah slab bridge

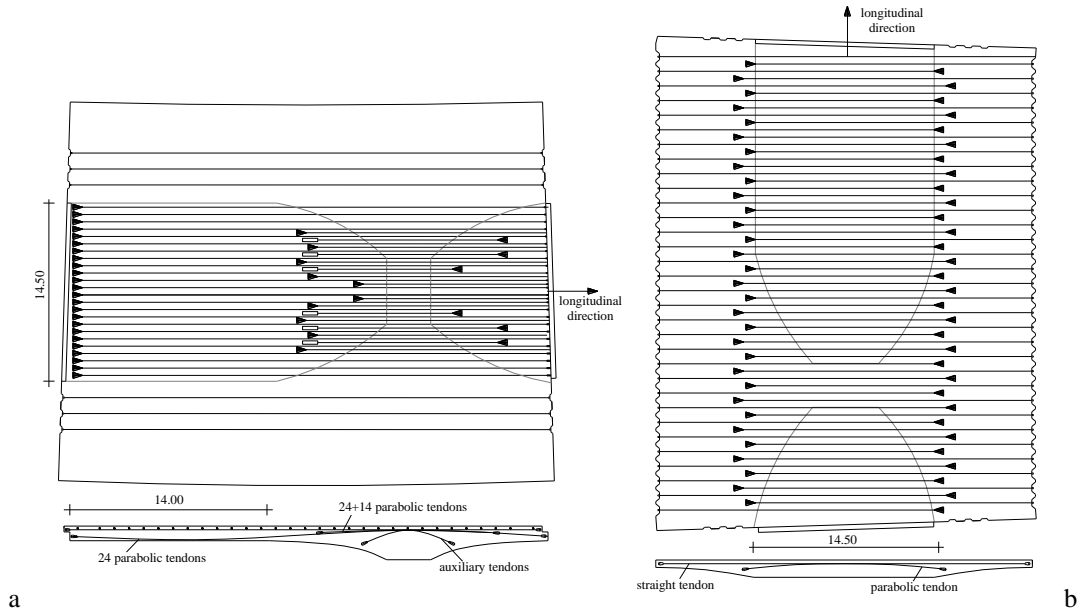


Fig. 14 Geometry of the first Jeddah slab bridge (dimensions in [m]); (a) plan and longitudinal view of the deck; (b) plan and transverse view of the deck

compressed. Through prestressing a uniform compressive stress is obtained within each slab cross section. For live loads the tensile stresses due to bending moments (positive or negative) add to the uniform compressive ones due to prestressing, with small values of temporary tensions allowed.

Summarizing, the following design choices were considered:

- null deflections due to bending moments are imposed null for dead loads and prestressing.
- Uniform compressive stresses in every cross section for dead loads and prestressing; null value of tensile stresses for 50% of the maximum bending moment due to live loads.
- The maximum tensile stress ( $f_{ct} = f_{ctk}/\gamma_c$ ) is allowed for the worst value of a live load combination acting on the structure. Small values of tensile stresses are allowed but no crack opening is achieved. Micro-cracks only appear in a transient stage and the entire value of tension in the section must be faced by ordinary steel reinforcement.

The longitudinal profile is composed of two parts: the central one, for a length of 14.00 m, with a cross section of constant depth; the side one (next to the pier), with a variable depth.

The depth of the central part is constant ( $h=1.00$  m) and the tendon is parabolic. This part of the deck is halfway between two points where the bending moment is zero, so it can be considered as a simply supported beam with an effective rectangular cross section and a parabolic tendon. The load equivalent to prestressing  $q_p$  must be equal to the dead loads. Hence the prestressing force at time  $t = t_\infty$  is

$$P = \frac{M}{e_{\max}} = \frac{q_{dead} L^2}{8 e_{\max}} = \frac{q_{dead} L^2}{8 \left( \frac{h}{2} - d \right)} \quad (31)$$

From Eq. (31), the value of  $P=3,000$  kN was found for the longitudinal strip, 1.00 m wide.

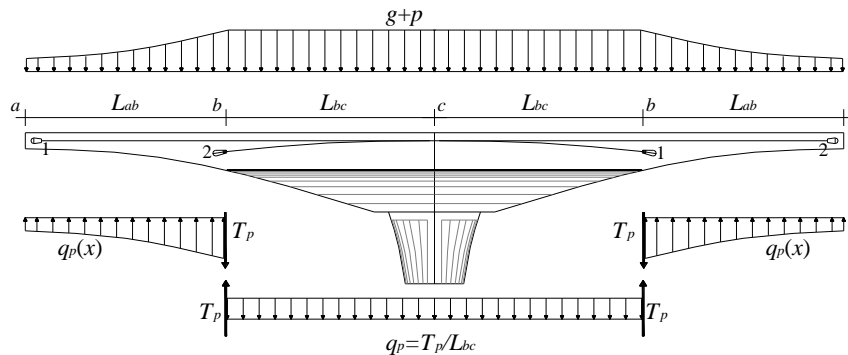


Fig. 15 Load balancing in the transverse direction

With this value of prestressing force the number and kind of tendons can be chosen for the central part of the span. In the central longitudinal strip (14.50 meters wide), 24 tendons with 19 strands of 0.5" were used.

For the longitudinal strip next to the pier, the case of parabolic tendons with variable depth of cross section was applied for load balancing. Keeping in mind that the value of prestressing axial force is already set, the shape of the cross section can be found by relation (25) in which  $h_0 = 1.00$  m,  $h(L) = 2.30$  m,  $\gamma = 25$  kN/m<sup>3</sup>,  $Q = 319$  kN,  $q = 3$  kN/m<sup>2</sup>. From Eq. (25) the new value of  $P = 5,000$  kN is found. So another 14 parabolic tendons have to be added to the previous 24, for a total of 38 tendons (Fig. 14(a)).

The chosen geometric shape and the prestressing make it possible to balance permanent loads and to have an average value of uniform compressive stress of about 3.0 MPa in each cross section, in service life after all dead loads have been applied. Auxiliary tendons were added next to the pier in order to face the local effect of shear forces due to live loads.

Three straight and centered tendons were added longitudinally at each side of the cantilever (12 strands, 0.5") for supplying an uniform compression, in order to reduce the cross section warping of the bridge deck and the shear lag effect and also to provide a hydrostatic effect on concrete.

For what concerns the transverse profile, the load balancing concept was applied through a straight tendon in the side cantilever part of the transverse section, with a variable depth. In the central part instead a constant depth with parabolic tendons was considered.

In order to find the expression that gives the shape, Eq. (19) was applied with  $Q = 0$ ,  $h_0 = 0.32$  m,  $h(L) = 1.00$  m,  $L = 7.50$  m. In this case the values of prestressing force  $P$  and coefficient  $\alpha$  were found for each transverse strip:  $P = 1,120$  kN/m,  $\alpha = 0.211$  m<sup>-1</sup>.

In Fig. 14(b) the layout of the transverse prestressing tendons is shown, while in Fig. 15 the conceptual design of the transverse section is clarified.

Consider the load balancing of the side cantilever part. The sudden variation of the center line slope in the section  $b$ , with a constant prestressing force, corresponds to a concentrated vertical force that for equilibrium, is equal to the shear force  $T_p$  due to the non-uniform dead loads applied. So, by considering the sum of dead loads and prestressing equivalent loads, the cross section part of the deck with a catenary profile can be considered as perfectly balanced and subjected only to a compressive uniform stress. The central part instead is subjected to dead loads and prestressing downward equivalent loads and the result is that the load acting on the cantilever is transferred to the central part. This is correct if the two lengths  $L_{ab}$  and  $L_{bc}$  are equal. Hence the central

longitudinal strip, 14.50 meters wide, is subjected to a uniform distributed load, due to the side cantilevers whose dead loads are perfectly balanced by the longitudinal prestressing. Moreover the resultant downward load per square meter on this central strip can be balanced by the longitudinal prestressing, which represents an upward equivalent load, as seen above. In the transverse direction, the mean compressive uniform stress is about 2.0 MPa and in this way every concrete element is compressed in each direction, enhancing structural performance in terms of durability.

The prestressing force in the longitudinal direction has a healthy effect on the Gerber saddles, which are a critical point for the durability of these bridges. Indeed, the load balancing makes it possible to eliminate the permanent elastic deflections and the related delayed deformations due to creep. Hence relative rotations in the internal hinges supplied by the Gerber saddles only occur for live loads and the durability of these critical points is strongly enhanced.

### 6.2 Design for live loads

After the load balancing has been applied for permanent actions, the effects of live loads have to be taken into account. The main external actions to be considered in the design are those related to moving loads and temperature. Because the structure is axially statically determinate, due to the sliding bearings on the Gerber saddles, the temperature gradient has an effect on internal forces but the uniform change of temperature has none. Seeing the environmental conditions, a temperature gradient of 15°C was considered, with a warmer upper surface. For moving loads three lanes for each carriageway were considered, to apply traffic loads and a lane for pedestrians. In the original design the loads given by the code of the Arabian Ministry of Communication (MOC 1973) and the AASHTO standards (AASHTO 1977) were applied. For this evaluation instead the loads of Eurocode EC1 (CEN 2004) and the rules of EC2 for concrete bridges (CEN 2005) have been applied.

With the main aim of limiting concrete cracking under live loads, the design strategy was to limit tensile stresses to the value  $f_{ct} = 1.35$  MPa. This choice is also related to possible problems of fatigue, due to the repetition of live loads and micro-crack opening. Moreover, severe environmental conditions (salty and humid atmosphere of the lagoon) suggested having no cracks opening, always maintaining  $w < 0.1$  mm.

Consider now the transverse section with the live loads applied: the minimum section depth was chosen for technological reasons and limited to 0.32 m (section *a* of Fig. 15). The maximum one (section *b* of Fig. 15) was set to 1.00 m. For a transverse strip 1.00 m wide, the values  $N = 1,120$  kN/m,  $M_{live} = 300$  kNm/m,  $f_{ct} = 1.35$  MPa were considered.

In the longitudinal direction the minimum depth is the value of 1.00 m set above and the values of internal forces in the most stressed section are:  $N = 2,940$  kN/m,  $M_{live} = 702$  kNm/m. By setting a maximum allowable value of tensile stresses  $f_{ct} = 1.35$  MPa, Eq. (29) can be applied in each cross section and the limit field can be plotted. Moreover, by calculating the maximum and minimum bending moment diagrams, the eccentricity diagrams for the worst live loads combination can also be drawn. Here only the bending moment diagram for a single span is shown, considering the envelope of the max-min bending moments, obtained on the finite element model of the whole bridge.

Fig. 16 shows the evaluation of the compressive force line, as for the thrust line of a funicular arch, explaining the strategy illustrated in the previous sections. A comparison between the eccentricity diagrams of the compressive force and the limit field, for the longitudinal profile of the bridge, is shown by applying conditions (30), together with the sections in which there are the

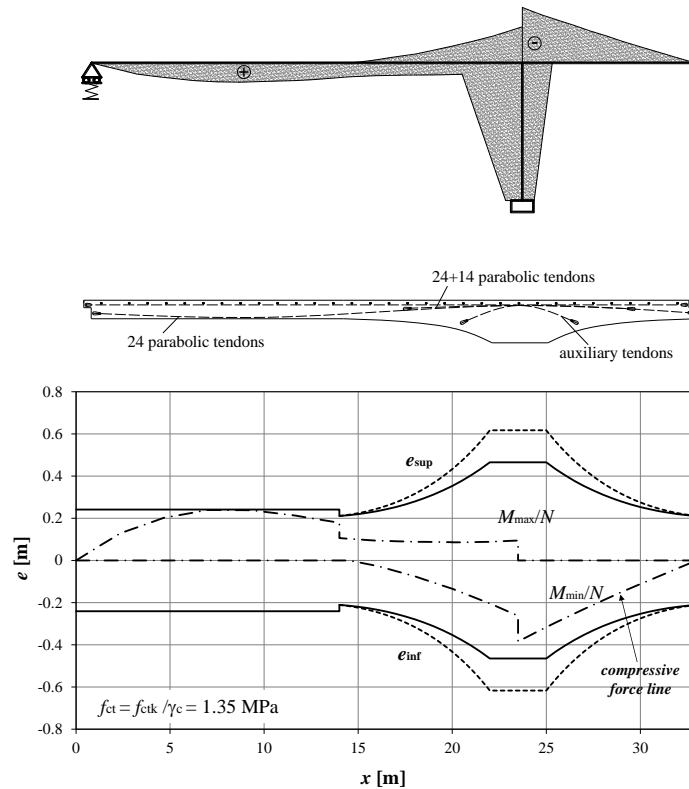


Fig. 16 Envelope diagram of bending moments due to live loads, longitudinal limit field and eccentricity diagrams for evaluations of safety against cracking

highest values of tensile stresses in service life. The continuous line refers to the limit field of a deck in which the double profile variation has been considered, while the dotted line refers to a deck with a single profile variation.

The construction stages due to the subsequent addition of new spans of the multispan bridge, do not modify the stress state because the structural subsequent construction of each span after the previous one, assures the flexural balancing of every span. Indeed, the low deformation value of the elastic support (Fig. 16) in the Gerber saddle, due to the load introduced by the new span built (load  $Q$  of Fig. 11), modifies the bending moment diagram in a negligible way, because the central span is highly deformable. Gerber saddles are placed in the points of the structure for which the equivalent continuous beam subjected to the same permanent loads, would present null values of bending moments.

Note that the jump in the limit field depends on the sudden axial force variation due to the change in the number of prestressing tendons (from 24 in the part with a constant depth to 38 in the part with variable shape).

In this way concrete cracks are avoided while tensile stresses are strongly limited and entirely faced by ordinary steel reinforcements.

Moreover, in this kind of structure there are no deformations due to dead loads because there is perfect balancing with prestressing, except for the axial strain due to the uniform compressive



Fig. 17 Bridge construction. (a) Casting by night, (b) Completed spans and continuous scaffolding for the formworks

stresses. But this is not a problem because the structure is axially statically determinate. Structural deflections and strains only depend on bending moments due to live loads. Hence strains could only appear in transient stages as tensile stresses and micro-cracks appear due to live loads. This is extremely important for the reduction of time-dependent strain effects, like those due to creep. When the deck is very wide, with long side cantilever parts, the creep-related strains increase the maximum deflections of the cantilever end due to dead loads. But by balancing permanent loads and prestressing the total applied load becomes zero and no deflections appear; temporary strains due to live loads are not affected by creep. Only the effect of the initial prestressing force, which is larger than the final one, at  $t_\infty$  after losses, is present with an upward displacement (as a pre-camber, useful to the formworks detachment at the initial time  $t = t_0$ ): it disappears after a few months.

Particular attention must be paid to Gerber saddles, which could be preferential ways for concrete degradation due to the waterproofing loss of the expansion joints. The relative rotations which are allowed in these points can increase due to time-dependent effects leading to joint misalignments. In the case of a load balanced structure instead, there are no rotations for dead loads, but only horizontal displacements due to the prestressing force, the uniform temperature change and the free shrinkage. Only small and temporary rotations appear under live loads, but these become zero when the moving load disappears.

### 6.3 Information on construction phase and evaluations after 30 years

This section refers to the general structural conditions of the Jeddah bridges (Arici and Granata 2009), about 30 years after their construction, and to the durability and degradation of the structures and of their elements.

These evaluations are helpful to establish the effectiveness of the designed solutions in order to limit degradation, through the load balancing concept.

The concrete used during construction was obtained through a careful mix-design, by using sulfate-resistant cement, basaltic aggregates, super-plasticizers and hardening retardant additives. After every cast careful checks on quality and strength were performed. Because of the very hot weather, the massive casts were made by night with water cooling (Fig. 17). A whole span was cast in a night to avoid discontinuities between different casts or construction joints. The concrete was carefully cured and initial cracking, due to the hydration heat, was avoided by applying initial appropriate moderate prestressing, introduced soon after the cast of a single span was completed.

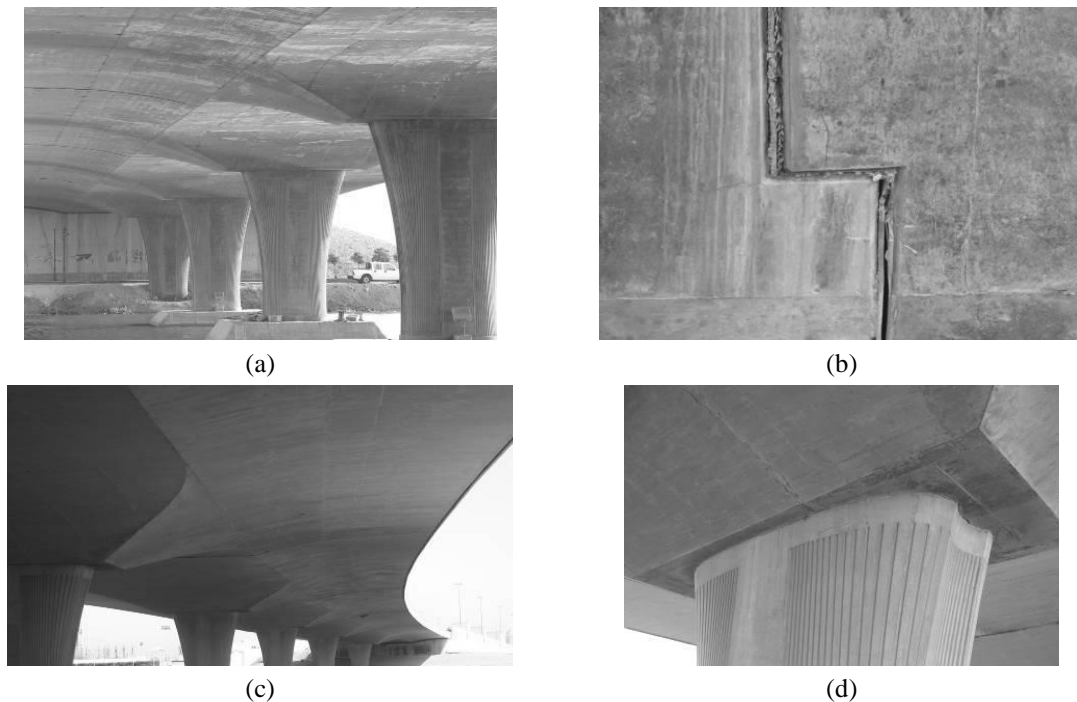


Fig. 18 Jeddah bridges today (a) view at the intrados of the deck over the sea, (b) the Gerber saddle, (c) view at the intrados of the first curved bridge, (d) view of the joint between the pier and the deck

About 30 years after construction, although no maintenance policy has been provided for these bridges, to the present authors' knowledge, the design criteria adopted, the good quality of the materials and the local workforces involved in construction, have led to the desired safety level, maintaining it in time.

A visual inspection allowed the authors to recognize the most important elements:

- No superficial clues of ordinary steel or prestressing corrosion were found (the inspection was conducted on the basis of methodologies similar to those used by Fuzier *et al.* 2005).

- No superficial detachments of reinforcement cover are found. Locally and along the conjunctions between the formworks, originally supported by continuous scaffolding, some reinforcement bars are externally evident very close to the deck intrados.

- Neither transverse nor longitudinal deflections nor strains due to time-dependent effects (creep, shrinkage, steel relaxation) can be seen. The longitudinal and transverse profiles appear perfectly aligned, with no deflections.

- No relative rotations are found in the Gerber saddles and no joint misalignments have been detected. Only one micro-crack can be seen along one saddle, probably due to the local effect of prestressing anchorage forces.

- There are no waterproofing losses of the joints.

- Cracks can be seen in the massive casts of the abutments (not prestressed), probably due to concrete shrinkage in the first stages of service life, but the crack widths give rise to no worry about steel corrosion.

Fig. 18 shows the present state of the bridges, in the most sensitive points of the structures.

## 7. Conclusions

A study has been presented on the conceptual design of prestressed concrete slab bridges through the one-way flexural load balancing concept. When the permanent load of a structure is balanced by prestressing, considered as an opposite external load, elastic deflections are compensated for and the global structural behavior is enhanced. This fact has an immediate and important consequence on delayed deflections due to creep, which are minimized. Hence the redistribution of stresses due to time-dependent phenomena can be avoided or strongly limited through appropriate use of prestressing.

The flexural load balancing concept has been applied to concrete slab bridges with variable depth and different layout of prestressing tendons. This design concept applied to slab bridges, allows to conjugate the static functionality with the structural outward shape. Indeed the correct static solution implied a natural aesthetic expressivity, drawing slender shapes in the space, which lighten the bridge, reducing the heaviness of concrete. The effectiveness of the proposed approach to structural design has been shown through the case study of the slab bridges built 30 years ago at Jeddah, Saudi Arabia, on a lagoon, in a critical environmental condition. The related discussion on aspects concerning full and partial prestressing, concrete cracking, delayed deformations and serviceability limit state can be useful for designers in considering the proposed approach as an up-to-date philosophy for the conceptual design of bridges.

## References

- Aalami, B.O. (1990), "Load balancing: a comprehensive solution to post-tensioning", *ACI Struct. J.*, **87**(6), 662-670.
- AASHTO (1977), *Standard specifications for Highway Bridges* 12th Ed., Association General Offices, Washington.
- Abeles, P.W. and Bardhan Roy, B.K. (2003), *Prestressed concrete designer's handbook*, 3rd Ed., 1981, reprinted 2003, Spon Press.
- Aguiló, M., Manterola, A.J., Onzain, M. and Rui-Wamba, J. (2004), *Javier Manterola Armisen, Pensamiento y obra*, (Javier Manterola Armisen. Concept and works), *Fund. Esteyco.*, Madrid..
- American Concrete Institute (ACI) (1997), *Prediction of creep, shrinkage, and temperature effects in concrete structures*, *ACI 209R-92*, reported by ACI Committee 209, 1-47, reapproved 1997.
- American Concrete Institute (ACI) (1999), *ACI425.5R-99 - State-of-the-Art Report on Partially Prestressed Concrete*, Reported by Joint ACI-ASCE Committee 423.
- American Concrete Institute (ACI) (2008), *209.2R08 Guide for modelling and calculating shrinkage and creep in hardened concrete*, reported by ACI Committee 209, 1-45.
- American Concrete Institute (ACI) (2012), *209.3RXX Time Dependent Effects in Concrete Structures*, preliminary draft reported by ACI Committee 209.
- Arenas, de P.J.J. (1974), "El pretensado considerado como accion compensadora de las cargas exteriores", ("Prestressing considered as an action compensating external loads"), *Revista de Obras Publicas*, **121** (3106), 97-113.
- Arici, M. (1985), "Ponte sulla laguna Ruwais a Gedda (Arabia Saudita)", ("Bridge over the Ruwais lagoon at Jeddah, Saudi Arabia"), *L'industria Italiana del Cemento*. n.12/85, 764-779, Pubblicemento, Roma.
- Arici, M. and Granata, M.F. (2007), "Analysis of curved incrementally launched box concrete bridges using Transfer Matrix Method", *Bridge Struct.*, **3**(3-4), 165-181.
- Arici, M. and Granata, M.F. (2009), "Durability evaluations on the bridge over the Ruwais lagoon at Jeddah", Beushausen H., *Concrete Repair, Rehabilitation and Retrofitting*, Balkema.

- Arici, M., Granata, M.F. and Recupero, A. (2011), "The influence of time-dependent phenomena in segmental construction of concrete cable-stayed bridges", *Bridge Struct.*, **7**(4), 125-137.
- Bernard-Gély, A. and Calgaro, J.A. (1994), *Conception of bridges* (in French: Conception des ponts), Presses de l'Ecole de Ponts et Chaussées.
- Bazant, Z.P. (1972), "Prediction of concrete creep effects using age-adjusted effective modulus method", *J. Am. Concrete Ins.*, **69**, 212-217.
- CEN (2004), EN 1991-2, *Traffic loads on bridges*, CEN, Bruxelles.
- CEN (2005), EN 1992-2, *Design of concrete structures - Concrete bridges - Design and detailing rules*, CEN, Bruxelles.
- Chiorino, M.A. (2005), "A Rational Approach to the Analysis of Creep Structural Effects", *Shrinkage and Creep of Concrete*, Gardner & Weiss Ed., ACI SP-227, 107-141, American Concrete Institute.
- Chiu, H., Chern, J. and Chang, K. (1996), "Long-term deflection control in cantilever prestressed concrete bridges I: control method", *J. Eng. Mech.*, ASCE, **122**(6), 489-494.
- Favre, R. and Burden, O. (1999), "Amount of prestressing based on serviceability requirements", *IABSE Symposium*, Rio de Janeiro, 594-601
- Favre, R. and Markey, I. (1994), "Generalization of the load balancing method", *Proceedings of The 12th FIP Congress*, Washington DC. USA.
- Fib (2012), *Bulletin d'Information n. 65 - Model Code 2010 - Final draft*, Volume 1, fib, Lausanne.
- Fuzier, J.P., Ganz, H.R. and Matt, P. (2005), fib (CEB-FIP) *Bulletin 33, Durability of post-tensioning tendons*, 1-71, fib, Lausanne.
- Ghali, A. and Tadros, M. (1985), "Partially prestressed concrete structures", *J. Struct. Eng.*, ASCE, **111**(8), 1846-1865.
- Gilbert, R.I. and Mickleborough, N.C. (2005), *Design of Prestressed Concrete*, Spoon Press.
- Granata, M.F., Margiotta, P., Arici, M. and Recupero, A. (2012a), "Construction stages of cable-stayed bridges with Composite deck", *Bridge Struct.*, IOS Press, **8**(3-4), 93-106.
- Granata, M.F., Margiotta, P., Recupero, A. and Arici, M. (2012b), "Partial elastic scheme method in cantilever construction of concrete arch bridges", *J. Bridge Eng.*, ASCE, **18**(7), 663-672.
- Granata, M.F., Margiotta, P. and Arici, M. (2013a), "A simplified procedure for evaluating the effects of creep and shrinkage on prestressed concrete girder bridges and the application of European and North-American prediction models", *J. Bridge Eng.*, ASCE, **18**(12), 1281-1297.
- Granata, M.F., Margiotta, P. and Arici, M. (2013b), "A parametric study of curved incrementally launched bridges", *Eng. Struct.*, **49**, 373-384.
- Granata, M.F., Margiotta, P., Recupero, A. and Arici, M. (2013c), "Concrete arch bridges built by lattice cantilevers", *Struct. Eng. Mech.*, **45**(5), 703-722.
- Granata, M.F. and Arici, M. (2013), "Serviceability of segmental concrete arch-frame bridges built by cantilevering", *Bridge Struct.*, **9**(1), 21-36.
- Guyon, Y. (1960), *Prestressed Concrete*, John Wiley and Sons, New York.
- Jirásek, M. and Bazant, Z.P. (2002), *Inelastic Analysis of Structures*, Chichester, J., Wiley and Sons.
- Khan, A.A., Pathak, K.K. and Dindorkar, N. (2010), "Cable layout design of one way prestressed concrete slabs using FEM", *J. Eng. Sci. Manag. Edu.*, **2**, 34-41.
- Khan, A.A., Pathak, K.K. and Dindorkar, N. (2013), "Cable layout design of two way prestressed concrete slabs using FEM", *Comput. Concrete*, **11**(1), 75-91.
- Kuyucular, A. (1991), "Prestressing optimization of concrete slabs", *J. Struct. Eng.*, ASCE, **117**(1), 235-254.
- Lee, D.H. and Kim, K.S. (2011), "Flexural strength of prestressed concrete members with unbonded tendons", *Struct. Eng. Mech.*, **38**(5), 675-696.
- Leonhardt, F. (1964), *Prestressed Concrete, Design and Construction*, W. Ernst & Sohn, Berlin.
- Leonhardt, F. (1980), *Vorlesingen über Massivbau*, Springer Verlag, Berlin.
- Leonhardt, F. (1986), *Ponts - Puentes*, Presses Polytechniques Romandes, Lausanne.
- Lin, T.Y. (1963), "Load balancing method for design and analysis of prestressed concrete structures", *J. Am. Concrete Ins.*, **60**(6), 719-742.
- Lin, T.Y. and Burns, N.H. (1982), *Design of Prestressed Concrete Structures*, John Wiley and Sons, New

York.

- Lin, T.Y. and Thornton, K. (1972), "Secondary moment and moment redistribution in continuous prestressed concrete beams", *PCI J.*, Jan-Feb., 8-20.
- Mathivat, J. (1979), *Incremental Construction of Prestressed-Concrete Bridges* (in French: Construction par encorbellement des ponts en beton précontraint), Editions Eyrolles.
- MOC (1973), *General specification for road and bridge construction*, Riyadh, MINCON.
- Naaman, A.E. (1980), "Partially prestressed beams: a unified design procedure for strength and serviceability", *Proceedings of the FIP Symposium on Partial Prestressing and Practical Construction in Prestressed and Reinforced Concrete*, Bucharest, Romania, 236-249.
- Naaman, A.E. (1985), "Partially prestressed concrete: review and recommendations", *J. Prestress. Concrete Ins.*, **30**(6), 30-71.
- Naaman, A.E. (1990), "A new methodology for the analysis of beams prestressed with unbonded or external tendons", *External Prestressing in Bridges, ACI SP-120*, American Concrete Institute, 339-354.
- Ng, P.L. and Kwan, A.K.H. (2006), "Practical determination of prestress tendon profile by load-balancing method", *Tran. Hong Kong Ins. Eng.*, **13**(3), 27-34.
- Oh, B.H. and Jeon, S.J. (2001), "Realistic equivalent load methods in prestressed concrete structures", *KCI Concrete J.*, **13**(1), 11-17.
- Recupero, A. and Granata, M.F. (2013), "Bending-shear interaction domains for externally prestressed concrete girders", *Adv. Civil Eng.*, Paper no. 580646, 1-12.
- Stern, I. (1999), "Optimization of prestressing tendon profile", *fib Symposium*, Prague.
- Strasky, J. (2003), "The power of prestressing", *Struct. Concrete Int.*, **4**(1), 25-43.
- Teixeira, A.O.F. and Assan, A.E. (1998), "Analysis of continuous prestressed slabs by the finite element method", *Computational Mechanics, New Trends and Applications*, Eds. Idelsohn, S., Oñate, E. and Dvorkin, E., CIMNE, Barcelona.
- Van der Molen, J.L. (1999), "Prestressed concrete design - Beyond load balancing", *Mech. Struct. Mater.*, Bradford, Bridge & Foster Editors, Balkema.
- Walther, R. (1982), "Partial prestressing, prestressed concrete of Switzerland", *Proceedings of The 9th FIP Congress*, Stockholm.